

## Analog-antianalog isospin mixing in $^{47}\text{K}$ $\beta^-$ decay

Brian Kootte<sup>1</sup>, H. Gallop<sup>1,3</sup>, C. Luktuke<sup>1,3</sup>, J. C. McNeil<sup>2,1</sup>, A. Gorelov<sup>1</sup>, D. G. Melconian<sup>1,4,5</sup>,  
 J. Klimo<sup>4,5</sup>, B. M. Vargas-Calderon<sup>4,5</sup> and J. A. Behr<sup>1,2,\*</sup>

<sup>1</sup>TRIUMF, 4004 Wesbrook Mall, Vancouver, B.C. V6T 2A3, Canada

<sup>2</sup>University of British Columbia, Department of Physics and Astronomy, 6224 Agricultural Road, Vancouver, B.C. V6T 1Z1, Canada

<sup>3</sup>University of Waterloo, Department of Physics and Astronomy, 200 University Ave W, Waterloo, Ontario N2L 3G1, Canada

<sup>4</sup>Cyclotron Institute, Texas A&M University, 3366 TAMU, College Station, Texas 77843-3366, USA

<sup>5</sup>Department of Physics and Astronomy, Texas A&M University, 4242 TAMU, College Station, Texas 77843-4242, USA



(Received 4 March 2024; accepted 3 May 2024; published 24 May 2024)

We have measured the isospin mixing of the  $I^\pi = 1/2^+$ ,  $E_x = 2.599$  MeV state in nearly doubly magic  $^{47}\text{Ca}$  with the isobaric analog  $1/2^+$  state of  $^{47}\text{K}$ . Using the TRIUMF atom trap for  $\beta$  decay, we have measured a nonzero asymmetry of the progeny  $^{47}\text{Ca}$  with respect to the initial  $^{47}\text{K}$  spin polarization, which together with the  $\beta$  asymmetry implies a nonzero ratio of Fermi to Gamow-Teller matrix elements  $y = 0.098 \pm 0.037$  for the  $1/2^+ \rightarrow 1/2^+$  transition. Interpreting  $y$  as mixing between this state and the isobaric analog state implies a Coulomb matrix element magnitude  $101 \pm 37$  keV. This relatively large matrix element supports a model from the literature of analog-antianalog isospin mixing, which predicts large matrix elements in cases involving excess neutrons over protons occupying more than one major shell. The result supports pursuing a search for time-reversal odd, parity-even, isovector interactions using a correlation in  $^{47}\text{K}$   $\beta$  decay.

DOI: [10.1103/PhysRevC.109.L052501](https://doi.org/10.1103/PhysRevC.109.L052501)

**Introduction.** The neutron beta decays to its isobaric analog state, the proton, as does tritium. Many other isotopes undergo beta minus decay to states of same spin  $I$  and parity  $\pi$ , but because of the extra Coulomb energy at higher  $Z$ , decay to the isobaric analog state is energetically forbidden. So the Gamow-Teller operator dominates, while the Fermi operator linking isobaric analog states is only allowed if some low-lying final state of the same  $I^\pi$  is mixed by an isospin-breaking interaction with the excited isobaric analog. We see such isospin breaking in an  $I^\pi = 1/2^+$  state in the  $^{47}\text{Ca}$  nucleus 80% fed by the beta decay of  $^{47}\text{K}$ . Interference between Gamow-Teller and isospin-suppressed Fermi amplitudes produces an asymmetry of the progeny recoil direction with respect to the initial nuclear spin, which we measure with TRIUMF's Neutral Atom Trap for  $\beta$  decay (TRINAT).

Since  $^{47}\text{Ca}$  and  $^{47}\text{K}$  are near closed shells, the single known  $^{47}\text{Ca}$   $1/2^+$  state may contain much of the antianalog configuration, and is predicted to have a relatively large Coulomb mixing matrix element with the analog [1]. Sensitivity to time reversal-odd parity-even (TOPE) inherently isovector [2]  $N$ - $N$  interactions through a  $\beta$ - $\nu$ -spin correlation is thought to be enhanced in these systems, as the small amount of time reversal is referenced to Coulomb rather than strong interactions [3], which motivates our measurement of isospin breaking in  $^{47}\text{K}$  decay.

**Theory and methods: Analog  $\mathcal{A}$ -antianalog  $\bar{\mathcal{A}}$  mixing.** The antianalog configuration has same spin and occupancy of spatial orbitals as the isobaric analog, but has total isospin reduced to  $T = T_z$ , with the antisymmetry of its wavefunction encoded differently between spin and isospin parts so that it is orthogonal to the analog state. Auerbach and Loc [1], using schematic wavefunctions, write for analog-antianalog Coulomb mixing for  $n_1$  and  $n_2$  excess neutrons over protons occupying orbitals  $j_1$  and  $j_2$ :

$$H_C = \langle \bar{\mathcal{A}} | V_C | \mathcal{A} \rangle = \frac{\sqrt{n_1 n_2}}{2T} (\langle j_1 | V_C | j_1 \rangle - \langle j_2 | V_C | j_2 \rangle) \quad (1)$$

$$\rightarrow 0.35 \frac{\sqrt{n_1 n_2}}{2T} \frac{Z}{A^{2/3}} \text{MeV}, \quad (2)$$

for harmonic-oscillator wavefunctions, a uniform charge distribution, and cases where neutrons occupy two major shells differing by one  $\hbar\omega$ . Reference [1], using experimental Coulomb energies from mirror nuclei, notes that Eq. (1) produces for occupancy of both the  $p_{3/2}$  or  $p_{1/2}$  and  $f_{5/2}$  or  $f_{7/2}$  subshells  $H_C$  about a factor of two smaller than the major shell occupancy Eq. (2), thus  $f_{7/2}$  is not a major shell when considering Coulomb energies. Reference [1] then benchmarks these simple expressions with random phase approximation (RPA) calculations to an accuracy of  $\approx 20\%$ . Equation (2) predicts  $H_C = 160$  keV for our case  $^{47}\text{K}^{28}$  (with  $n_1 = 8f_{7/2}$  neutrons and  $n_2 = 12s_{1/2}$  neutron excess over protons).

**Isospin-suppressed  $\beta$  decay.** In the angular distribution for allowed  $I = 1/2$   $\beta$  decay in terms of lepton momentum  $p$  and

\*behr@triumf.ca

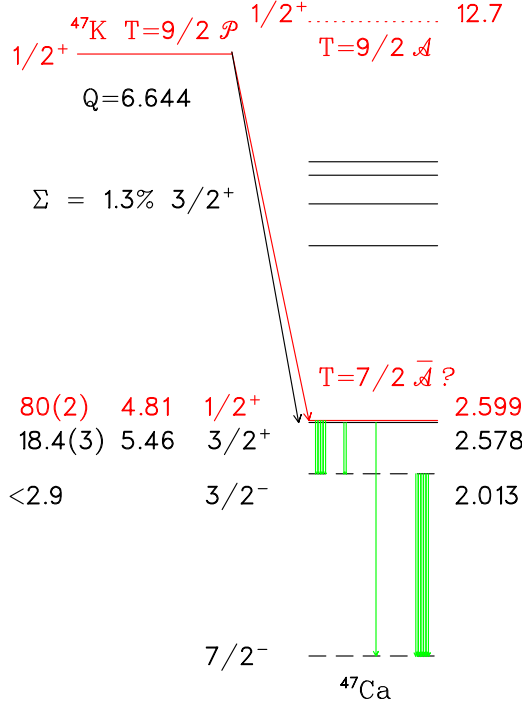


FIG. 1. Relevant allowed decay of  $^{47}\text{K}$ , showing  $\beta^-$  branches  $>0.04\%$ ,  $\log(ft)$ ,  $I^\pi$ , energy [MeV], and isospin  $T$  of the isobaric parent  $\mathcal{P}$ , analog  $\mathcal{A}$ , and possible antianalog  $\bar{\mathcal{A}}$ . Thickness of  $\gamma$  transitions  $>5\%$  indicate intensity.

energy  $E$  [4,5],

$$dW = F(E, Z)pE p_v E_v \left[ 1 + a \frac{\vec{p}_\beta}{E_\beta} \cdot \frac{\vec{p}_v}{E_v} + \hat{I} \cdot \left( A_\beta \frac{\vec{p}_\beta}{E_\beta} + B_v \frac{\vec{p}_v}{E_v} \right) \right], \quad (3)$$

isospin-suppressed Fermi decay alters the correlation coefficients from their Gamow-Teller values:

$$a = \frac{y^2 - 1/3}{y^2 + 1},$$

$$A_\beta = A_{\beta GT} + f(M_F), \quad (4)$$

$$B_v = -A_{\beta GT} + f(M_F),$$

with  $y = g_v M_F / g_A M_{GT}$  and  $f(M_F) = 2\sqrt{I/(I+1)}y/(1+y^2)$ . The recoil asymmetry  $A_{\text{recoil}}$  is then proportional to  $A_\beta + B_v$ , which vanishes when  $M_F = 0$ . (Analytic expressions for the proportion, which are possible if the Fermi function is set to unity, are given in Refs. [6,7]; we compare here entirely to numerical simulations.)

$^{47}\text{K}$  and its  $\beta^-$  decay to  $^{47}\text{Ca}$ . The  $^{47}\text{K}$   $I^\pi = 1/2^+$  ground-state has magnetic moment  $1.933(9) \mu_N = 0.69 \mu_{\text{proton}}$  [8], suggesting a large fractional component of single-particle  $2s_{1/2}$ . The 80%  $\beta^-$  branch to the  $1/2^+$  2.599 MeV state (Fig. 1) has  $\log(ft) = 4.81$ , for which a literature shell-model calculation of the Gamow-Teller strength finds  $\log(ft)_{GT} = 4.39$  [9]. This experimental  $g_A |M_{GT}| = 0.305$  is considerably

TABLE I. Systematic uncertainties. Both observables are statistics dominated. NA denotes not applicable. Listed common systematics are so different between observables that we are not concerned with their correlation.

Source	$A_{\text{recoil}}$	pseudo $A_\beta$
$A_{\text{recoil}}$ bkg $6 \pm 4\%$	0.014	$<0.002$
Polarization $0.96 \pm 0.04$	0.004	0.023
$\beta^-$ branching ratio	0.002	0.022
Weak magnetism	0.0006	0.0003
Fit range in $Z \pm 20$ to 34 mm	0.012	NA
$^{47}\text{Ca}^{+1}$ percent bkg	0.001	NA
$^{47}\text{Ca}^{+N}$ distribution from TOF	$<0.0005$	NA
$E$ field	Negligible	0.025
Backscatter correction $-0.012 \pm 20\%$	NA	0.0024
Fit statistics	0.037	0.082
Total	0.041	0.091

smaller than the single-particle  $2s_{1/2}$   $GT$  value of  $\sqrt{3}$ . We include in our simulations the  $18.4 \pm 0.3\%$  branch to the 2.578 MeV first-excited  $3/2^+$  state, and another 1.3% known to decay to five other  $3/2^+$  states [10]; these can have no Fermi component so simply dilute our measured  $A_{\text{recoil}}$ . For pure Gamow-Teller decay, the  $\beta^-$  asymmetry  $A_{\beta GT} = -1/(I_i + 1) = -2/3$  for the  $1/2^+ \rightarrow 1/2^+$  transition and  $I_i/(I_i + 1) = +1/3$  for the  $1/2^+ \rightarrow 3/2^+$  transitions, so the precision of their average  $A_{\beta GT} = -0.467 \pm 0.020$  is needed to extract  $M_F$  from  $A_\beta$ .

Reference [10] also observes a total of 0.042% to first-forbidden branches. Although these can have asymmetries near unity, we can safely ignore them at our achieved accuracy. The experimental upper limit for direct  $\beta$  decay to the 2.013 MeV first  $3/2^-$  state would increase our uncertainty from branching ratios in Table 1 by a factor of 1.5. We constrain this branch with a calculation of the first-forbidden nonunique  $fT$  value [9] of 0.25%; our assignment of 0.25% uncertainty does not perturb our uncertainty.

*Experiment: TRIUMF neutral atom trap.* Figure 2 is a side view of the detection apparatus of TRIUMF's Neutral Atom Trap for  $\beta$  decay (TRINAT). Not shown is the collection trap from a vapor cell cube, nor the push beams between traps [11].

Using  $6 \times 10^6 \text{ s}^{-1}$  mass-separated  $^{47}\text{K}$  delivered from the TRIUMF-ISAC isotope separator online facility, we trapped on average 500–1000  $^{47}\text{K}$  atoms during the data-taking time. We optimized the number of atoms when the trapping light was tuned about three linewidths to the red of the  $4S_{1/2}$  to  $4P_{3/2}$   $F = 1$  to  $F = 2$  transition, as measured with respect to the optical resonance measured by Ref. [8]. Repumping light on the  $F = 0$  to  $F = 1$  transition was provided by 3.3 GHz fiber-coupled electro-optic modulators.

*Polarization by optical pumping.* The optical pumping scheme is similar to our  $^{37}\text{K}$  measurement [12]. Changes include much thinner pellicle mirrors (4  $\mu\text{m}$  polyimide with 100 nm Au coatings) along the optical pumping axis to reduce  $\beta$  straggling.

We alternate 2.9 ms trapping with 1.1 ms optical pumping, during which we make the polarized  $\beta$  decay measurements.

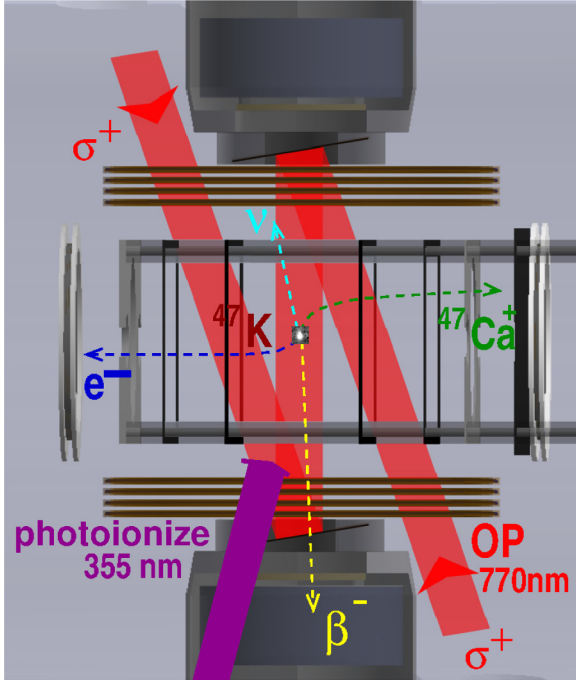


FIG. 2. TRINAT during the optical pumping time. Shown are  $\beta$  telescopes, mirrors for optical pumping light and its beams, magnetic-field coils, electric-field electrodes, and microchannel plates for electron and ion detection. A CMOS camera image of 1000 trapped atoms is superimposed. Distance between trap cloud and ion MCP is 9.7 cm.

During the polarization time, we switch the magnetic field from the trap's quadrupole to a uniform 1 gauss field pointed up, and apply circularly polarized light along the quantization axis. Once we start the optical pumping cycle, atoms increase spin to maximum, then stop absorbing the  $S_{1/2}$  to  $P_{1/2}$  light. If instead the light is linearly polarized, atoms keep absorbing, and the atoms and nuclei remain unpolarized.

Once excited, pulsed 355 nm light has enough energy per photon to photoionize from the  $P$  states about  $1/10^6$  atoms per pulse, detected in the ion microchannel plate (MCP) detector. The photoions, distinguished by their time-of-flight (TOF) and center position, determine average trap cloud sizes and positions when the magneto-optical trap (MOT) light is on.

The vanishing of photoion rate during the polarization time is then our probe of the atomic polarization quality. We measured 11 photoions while linearly polarized (about 1/4 the total beam time) and 1 photon circularly polarized (see Fig. 3). The polarization extracted by rate equations from this circular/linear ratio is independent of power and detuning of the optical pumping light to well within this accuracy. The fraction of nuclear polarization achieved for the decaying  $^{47}\text{K}$  atoms was  $P = \langle I_z \rangle / I = 0.96 \pm 0.04$ .

*Geometry and detectors.* An electric field collects  $^{47}\text{Ca}$  ions produced in  $^{47}\text{K}$   $\beta^-$  decay to an MCP with 78 mm active diameter located 9.7 cm away. By comparing trajectories with a detailed finite-element calculation, we found our simulations could assume a uniform 650 V/cm field. Decay by  $\beta^-$  naturally makes  $^{47}\text{Ca}^{+1}$  ions. Additional low-energy atomic

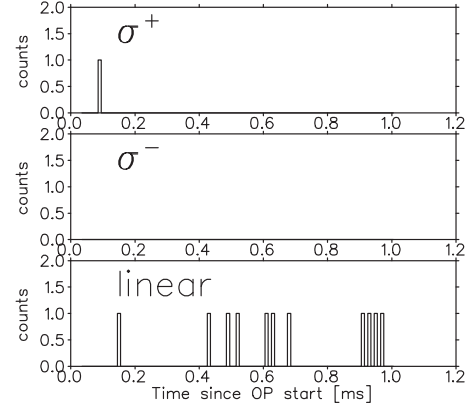


FIG. 3. Excited-state population during the optical pumping time for circularly and linearly polarized light. See text for deduction of nuclear polarization.

shake-off electrons, which take an average of 6 ns to reach the opposite 40 mm diameter MCP, provide a starting trigger for the TOF of  $^{47}\text{Ca}^{+2}$  and higher.

Critical to  $\beta$  detection is discriminating  $\beta$  from  $\gamma$ , because their ratio in  $^{47}\text{K}$  decay is about one to two. We use the same 0.30-mm-thick double-sided silicon strip detectors as Ref. [13], similarly requiring both  $X$  and  $Y$  strips above energy threshold and similar calibrated energy deposited. Our plastic  $4 \times 9$  cm<sup>2</sup> scintillators for  $\beta^+$  detection now use silicon photomultiplier (SiPM) readout, characterized in Ref. [14].

*Results:  $e^-$  recoil  $^{47}\text{Ca}$  ion coincidences.* Our most sensitive channel detects coincidences between decay recoils on the ion MCP and shake-off electrons on the  $e^-$  MCP. The TOF spectrum in Fig. 4 has contributions from  $^{47}\text{Ca}$  charge states +2 through +7. Their position asymmetry along the polarization axis is shown to be nonzero in Fig. 5, directly implying a nonzero Fermi contribution to the  $1/2^+ \rightarrow 1/2^+$  transition. (Since  $\beta^-$  decay makes +1 ions without shake-off, the  $e^-$ — $^{47}\text{Ca}$  events consistent with  $^{47}\text{Ca}^{+1}$  TOF are from  $\beta$

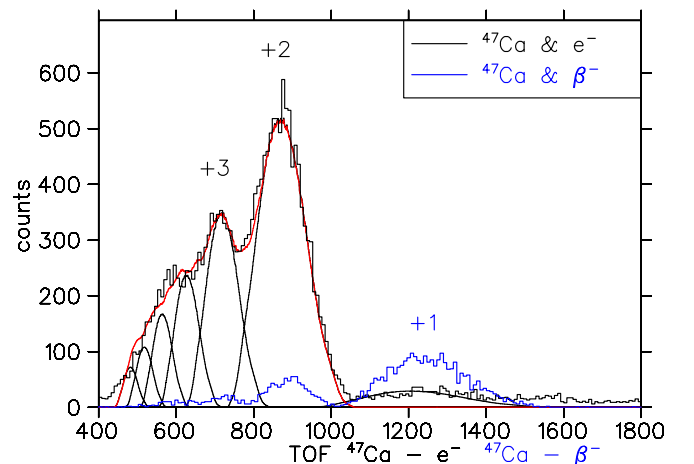


FIG. 4. Time-of-Flight (TOF) of  $^{47}\text{Ca}$  +2 to +7 ions started by shake-off  $e^-$ , showing the modeled data decomposition. Blue histogram: TOF started by  $\beta$  in the  $\Delta E$ - $E$  telescopes, which have lower statistics but less background from untrapped atoms and accidentals.

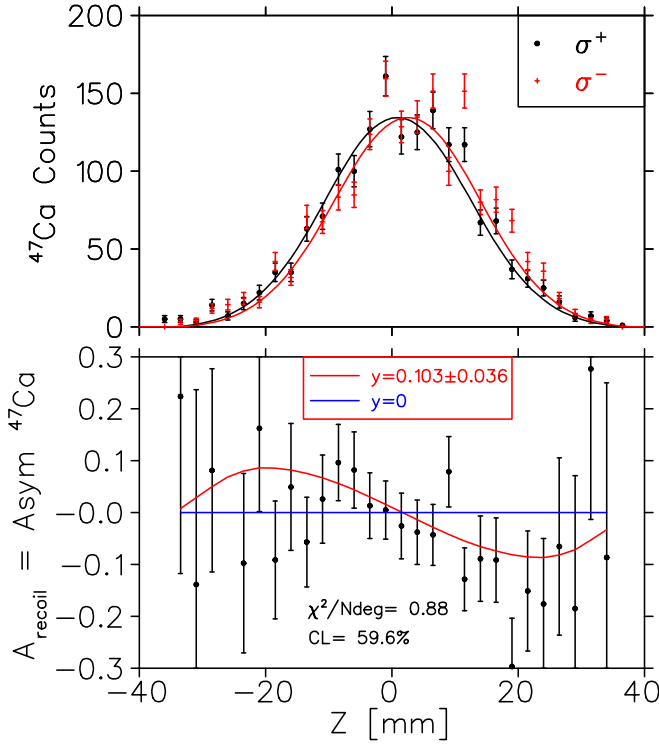


FIG. 5. (Top) Distribution along polarization axis  $Z$  of  $^{47}\text{Ca}^{+2,\dots,7}$  in coincidence with shake-off  $e^-$  for the two polarizations. (Bottom) The asymmetry of these distributions  $A_{\text{recoil}}$ , i.e., the difference divided by the sum of the top distributions. The nonzero asymmetry scales with  $y$  and directly implies a nonzero Fermi contribution.

and  $\gamma$  firing the  $e^-$  MCP and accidentals, so we do not use them for  $A_{\text{recoil}}$ .)

We model this by a numerical integration of  $\beta$  and  $\nu$  [Eqs. (1) and (2)], with the resulting  $^{47}\text{Ca}$  ions collected to the ion MCP by the uniform 650 V/cm electric field. We find it adequate to include the momentum perturbation on the  $^{47}\text{Ca}$  from a single 2 MeV  $\gamma$  subsequently emitted isotropically—note emission of the dominant  $\gamma$  in Fig. 1 must be isotropic. The result is  $y = +0.103 \pm 0.041$  (a solution with  $y \approx 10$  is physically excluded). Systematic uncertainties are listed in Table I.

*Backgrounds from untrapped atoms.* The vacuum-limited trap half-life of 10 s and the  $t_{1/2} = 17.5$  s of  $^{47}\text{K}$  implies that more than half the nuclei decay after the atoms leave the trap. We have measured this background with 1 hour of data while deliberately ejecting atoms from the trap. We deduce a background of  $6\% \pm 4\%$  of the events in the  $e^-$ - $^{47}\text{Ca}$  channel, roughly flat in TOF in the region we use of +2 through +7 charge states, and include that background in our simulation. This is consistent with a small fraction of the untrapped atoms sticking to the glassy carbon electrodes close to the trap, while shake-off electrons from other surfaces are excluded from the electron MCP by the electric field. Our  $\beta$  collimation is sufficient that we see backgrounds consistent with zero for the  $\beta$ -recoil channel considered below.

*$\beta$ -recoil coincidences using pseudo  $A_\beta$ .* We also measure  $\beta$  in coincidence with  $^{47}\text{Ca}$  recoils. If we measured  $^{47}\text{Ca}$  recoils

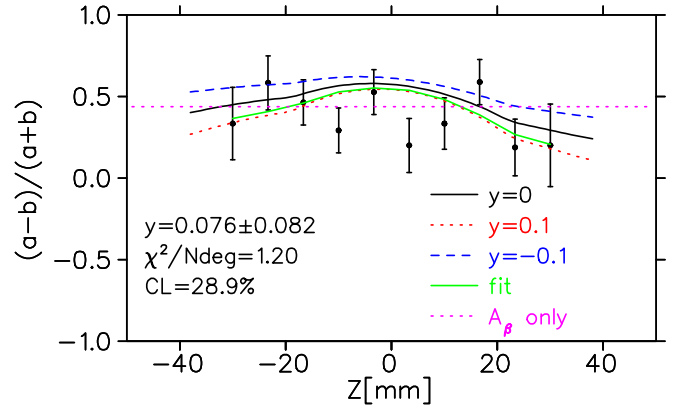


FIG. 6. Similar to Fig. 5, but for  $\beta$ - $^{47}\text{Ca}^{+1}$  coincidences.

over all directions and momenta, this would be a measurement of  $A_\beta$ . However, some  $^{47}\text{Ca}^{+1}$  ions with high transverse momenta do not impact the MCP, perturbing the asymmetry of  $\beta$  in coincidence by a well-defined combination of the  $\beta$ - $\nu$  correlation and the  $\nu$  asymmetry.

This observable, which we name pseudo  $A_\beta$ , we also model by numerical integration, including the effects of a single 2 MeV  $\gamma$ . We group the four combinations of  $\beta$  detector and polarization sign in pairs to cancel asymmetries, denoted “a” and “b” in Fig. 6. Numerical simulations for three values of  $M_F/M_{GT}$  show sensitivity to the asymmetry along with the best fit. A single straight line for  $M_F = 0$  and hypothetical full collection of  $^{47}\text{Ca}$  is shown to indicate how the asymmetries are distorted from  $A_\beta$ . The significantly smaller difference in asymmetry for positive vs negative  $Z$  is due to 0.22 and 0.45 mm displacements in the cloud  $Z$  and horizontal position and subsequent change in  $^{47}\text{Ca}$  collection, and is well-reproduced by the simulation.

We note that the sign of  $A_\beta$  is determined from this observable. We use this to determine the sign of our spin polarization.

To deduce  $y$  from pseudo  $A_\beta$  requires more precision and accuracy than  $A_{\text{recoil}}$  because of the nonzero  $A_{\beta GT} = -0.467$ . The uncertainties are summarized in Table I. Based on our previous  $^{37}\text{K}$   $A_\beta$  measurement [13], we scale our experimental value by 1/1.023 to approximately account for backscatter, assigning here a more generous uncertainty of 20% because we have not done full simulations of geometry changes.

The result from pseudo  $A_\beta$ ,  $y = 0.076 \pm 0.091$ , is consistent in sign with  $A_{\text{recoil}}$ , but with larger uncertainty.

*Recoil order corrections.* We use Refs. [5,15] for the correction from the recoil kinetic energy, the first-order in recoil correction from weak magnetism  $b_W$ , and the Coulomb finite-size correction. Assuming the wavefunction of initial and final  $1/2^+$  states is an  $s_{1/2}$  nucleon,  $b_W$  has no orbital angular-momentum contribution and becomes the nucleon value [16]: the first-class induced tensor  $d_l$  also vanishes for  $s_{1/2}$ . Similarly assuming single-particle  $s_{1/2} \rightarrow d_{3/2}$  for the 20% branches to  $3/2^+$  states, the orbital correction to  $b$  is zero if  $l$  changes; here we ignore potentially nonzero  $d_l$  and second-order in recoil corrections because of the 20% fraction. The recoil corrections increase our deduced  $A_{\text{recoil}}$  by

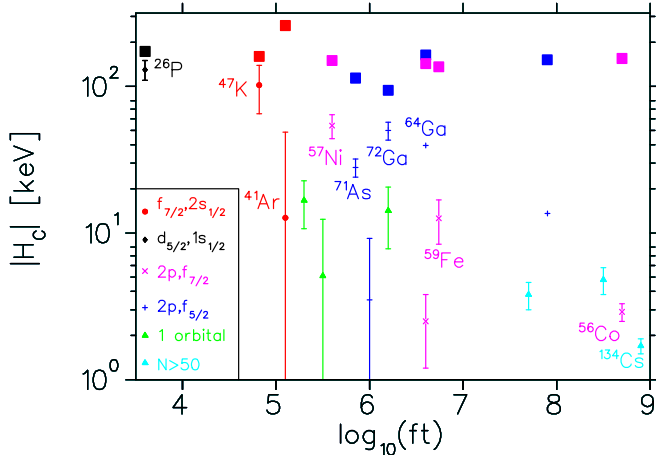


FIG. 7. Effective Coulomb mixing matrix element  $H_C$  as a function of  $\log(ft)$  for isospin-suppressed  $\beta$  decay (Refs. [17,20–26]). Solid squares are  $\mathcal{A}$ - $\bar{\mathcal{A}}$  mixing from Eq. (2) for  $^{47}\text{K}$  decay's  $N = 20$  shell crossing, Eq. (1) for  $^{26}\text{P}$  assuming  $d_{5/2}1s_{1/2}$  excess proton occupancy, and the approximate use of Eq. (1) [i.e., Eq. (2) divided by two] for all others [1].

0.0025, 0.0012 from  $b_W$  to which we assign 50% uncertainty; the Coulomb finite-size correction decreases  $A_{\text{recoil}}$  by 0.0017. Similarly,  $b_W$  changes pseudo $A_\beta$  by  $0.0006 \pm 0.0003$ .

**Result and isospin breaking.** Our weighted average of results from  $A_{\text{recoil}}$  and pseudo $A_\beta$  is then  $y = g_V M_F / g_A M_{GT} = 0.098 \pm 0.037$  for the  $1/2^+$  to  $1/2^+$  transition.

Given the measured  $g_A M_{GT} = 0.305$ , we deduce  $|M_F| = 0.030 \pm 0.011$  (assuming  $g_V = 1.00$ , and that we do not know the sign of  $M_{GT}$ ). To compare with other nuclei thought to be dominated by  $\mathcal{A}$ - $\bar{\mathcal{A}}$  mixing, we use a first-order perturbation theory expression from the literature [17,18]:  $M_F = \frac{\langle \mathcal{A} | H_C | \bar{\mathcal{A}} \rangle}{\Delta E} \sqrt{(T \mp T_z)(T \pm T_z + 1)}$  (upper vs lower sign for  $\beta^-$  vs  $\beta^+$ , respectively), along with the measured  $\bar{\mathcal{A}}$ - $\mathcal{A}$  splitting  $\Delta E = 10.1$  MeV [19], to deduce a Coulomb matrix element  $|H_C| = 101 \pm 37$  keV.

This Coulomb matrix element is over half of the 160 keV prediction of  $\mathcal{A}$ - $\bar{\mathcal{A}}$  mixing. We attribute this to the simple structure of nearly doubly magic  $^{47}\text{Ca}$  and its single  $1/2^+$  state. That this is not the full prediction suggests the state is somewhat more complex than  $\bar{\mathcal{A}}$ .

Many  $\beta$  decays in such systems have much smaller Coulomb matrix elements and  $M_F$ . Reference [1] suggests

the  $\bar{\mathcal{A}}$  configuration is often fragmented among many states. Figure 7 shows measurements of  $|H_C|$  with estimates from  $\mathcal{A}$ - $\bar{\mathcal{A}}$  mixing as a function of  $\log(ft)$ , a measure of nuclear complexity. Although more complete calculations have difficulties reproducing its large  $H_C$ ,  $^{26}\text{P}$  [26] has a large fraction of Eq. (1)'s  $\mathcal{A}$ - $\bar{\mathcal{A}}$  prediction if  $1d_{5/2}1s_{1/2}$  proton occupancy is naively assumed. There are several cases with neutron excess in both  $2p$  and  $1f$  orbitals with relatively large  $M_F$  and  $H_C$ , factors of two to four smaller than their  $H_C$  predictions from Eq. (1) [1]. In contrast, the  $\beta^+$  decay of  $^{56}\text{Co}$  has a strikingly small  $H_C$  given its relevant isobaric parent ( $\mathcal{P}$ )  $^{56}\text{Fe}$  also has excess neutrons spanning the  $N = 28$  shell closure: one explanation would be fragmentation of the  $\bar{\mathcal{A}}$  configuration. Cases with excess neutrons all in one orbital tend to have smaller  $H_C$ , consistent with little  $\mathcal{A}$ - $\bar{\mathcal{A}}$  mixing, although the most striking trend is the general drop of  $|H_C|$  with  $GT$  strength.

Reference [3] proposed a time-reversal measurement in  $|y| = 0.21 \pm 0.01$   $^{134}\text{Cs}$ , which has a very small  $M_{GT}$  and small Coulomb matrix element. A measurement was similarly pursued in  $|y| = 0.13 \pm 0.02$   $^{56}\text{Co}$  [27]. Such time-reversal  $\beta$  decay observables are proportional to  $y$ . For isovector TOPE nucleon-nucleon [28] matrix elements having similar dependence on nuclear complexity (e.g., a long-ranged isovector Yukawa could be similar to Coulomb), a faster decay like  $^{47}\text{K}$  with its large  $\bar{\mathcal{A}}$  component and its sizable  $y$  could also be a favorable system for a time-reversal search.

**Conclusion.** For the  $^{47}\text{K}$   $\beta^- 1/2^+ \rightarrow 1/2^+$  transition, we have measured the ratio of Fermi to Gamow-Teller matrix elements  $y = 0.098 \pm 0.037$ , and from the known  $GT$  strength we deduce  $|M_F| = 0.030 \pm 0.011$ . Interpreted as  $\mathcal{A}$ - $\bar{\mathcal{A}}$  mixing in the progeny  $^{47}\text{Ca}$ , this result implies a relatively large effective Coulomb mixing matrix element magnitude  $101 \pm 37$  keV. A large matrix element of 160 keV is generated for  $^{47}\text{Ca}$  from  $\mathcal{A}$ - $\bar{\mathcal{A}}$  mixing, as its excess neutrons over protons occupy two major shells,  $f_{7/2}$  and  $sd$ , with naturally different Coulomb energies [1]. The large fraction observed of that prediction we attribute to the existence of only one  $1/2^+$  state in the nearly doubly magic  $^{47}\text{Ca}$  [10].

**Acknowledgments.** We acknowledge TRIUMF-ISAC staff, in particular for  $\text{UC}_x$  target preparation. Supported by the Natural Sciences and Engineering Research Council of Canada and RBC Foundation, TRIUMF receives federal funding via a contribution agreement through the National Research Council of Canada.

- [1] Naftali Auerbach and Minh-Loc Bui, Coulomb corrections to Fermi beta decay in nuclei, *Nucl. Phys. A* **1027**, 122521 (2022).
- [2] M. Simonius, Constraints on parity-even time reversal violation in the nucleon-nucleon system and its connection to charge symmetry breaking, *Phys. Rev. Lett.* **78**, 4161 (1997).
- [3] A. Barroso and R. Blin-Stoyle, A test for time-reversal violation in allowed isospin-hindered beta-decay, *Phys. Lett. B* **45**, 178 (1973).
- [4] J. D. Jackson, S. Treiman, and H. Wyld, Coulomb corrections in allowed beta transitions, *Nucl. Phys.* **4**, 206 (1957).

- [5] B. R. Holstein, Recoil effects in allowed beta decay: The elementary particle approach, *Rev. Mod. Phys.* **46**, 789 (1974).
- [6] J. R. A. Pitcairn, D. Roberge, A. Gorelov, D. Ashery, O. Aviv, J. A. Behr, P. G. Bricault, M. Dombisky, J. D. Holt, K. P. Jackson, B. Lee, M. R. Pearson, A. Gaudin, B. Dej, C. Höhr, G. Gwinner, and D. Melconian, Tensor interaction constraints from  $\beta$ -decay recoil spin asymmetry of trapped atoms, *Phys. Rev. C* **79**, 015501 (2009).
- [7] S. B. Treiman, Recoil effects in  $K$  capture and  $\beta$  decay, *Phys. Rev.* **110**, 448 (1958).

- [8] F. Touchard, P. Guimbal, S. Büttgenbach, R. Klapisch, M. De Saint Simon, J. Serre, C. Thibault, H. Duong, P. Juncar, S. Liberman, J. Pinard, and J. Vialle, Isotope shifts and hyperfine structure of  $^{38-47}\text{K}$  by laser spectroscopy, *Phys. Lett. B* **108**, 169 (1982).
- [9] P. Choudhary, A. Kumar, P. C. Srivastava, and T. Suzuki, Structure of  $^{46,47}\text{Ca}$  from the  $\beta^-$  decay of  $^{46,47}\text{K}$  in the framework of the nuclear shell model, *Phys. Rev. C* **103**, 064325 (2021).
- [10] J. K. Smith, A. B. Garnsworthy, J. L. Pore, C. Andreoiu, A. D. MacLean, A. Chester, Z. Beadle, G. C. Ball, P. C. Bender, V. Bildstein, R. Braid, A. D. Varela, R. Dunlop, L. J. Eviatts, P. E. Garrett, G. Hackman, S. V. Ilyushkin, B. Jigmeddorj, K. Kuhn, A. T. Laffoley *et al.*, Spectroscopic study of  $^{47}\text{Ca}$  from the  $\beta^-$  decay of  $^{47}\text{K}$ , *Phys. Rev. C* **102**, 054314 (2020).
- [11] T. B. Swanson, D. Asgeirsson, J. A. Behr, A. Gorelov, and D. Melconian, Efficient transfer in a double magneto-optical trap system, *J. Opt. Soc. Am. B* **15**, 2641 (1998).
- [12] B. Fenker, J. A. Behr, D. Melconian, R. M. A. Anderson, M. Anholm, D. Ashery, R. S. Behling, I. Cohen, I. Craiciu, J. M. Donohue, C. Farfan, D. Friesen, A. Gorelov, J. McNeil, M. Mehlman, H. Norton, K. Olchanski, S. Smale, O. Thériault, A. N. Vantghem *et al.*, Precision measurement of the nuclear polarization in laser-cooled, optically pumped  $^{37}\text{K}$ , *New J. Phys.* **18**, 073028 (2016).
- [13] B. Fenker, A. Gorelov, D. Melconian, J. A. Behr, M. Anholm, D. Ashery, R. S. Behling, I. Cohen, I. Craiciu, G. Gwinner, J. McNeil, M. Mehlman, K. Olchanski, P. D. Shidling, S. Smale, and C. L. Warner, Precision measurement of the  $\beta$  asymmetry in spin-polarized  $^{37}\text{K}$  decay, *Phys. Rev. Lett.* **120**, 062502 (2018).
- [14] M. Ozen, J. A. Behr, M. Khoo, F. Klose, A. Gorelov, and D. Melconian, Lineshape response of plastic scintillator to pair production of 4.44 MeV  $\gamma$ s, *Nucl. Instrum. Methods Phys. Res. Sect. A* **1055**, 168490 (2023).
- [15] B. R. Holstein, Erratum: Recoil effects in allowed beta decay: The elementary particle approach, *Rev. Mod. Phys.* **48**, 673 (1976).
- [16] X. B. Wang and A. C. Hayes, Weak magnetism correction to allowed  $\beta$  decay for reactor antineutrino spectra, *Phys. Rev. C* **95**, 064313 (2017).
- [17] S. Bhattacharjee, S. Mitra, and H. Padhi, Fermi matrix elements in allowed beta transitions in  $^{56}\text{Co}$ ,  $^{58}\text{Co}$ , and  $^{134}\text{Cs}$ , *Nucl. Phys. A* **96**, 81 (1967).
- [18] S. D. Bloom, Isotopic-spin conservation in allowed  $\beta$ -transitions and Coulomb matrix elements, *Nuovo Cimento* **32**, 1023 (1964).
- [19] T. Burrows, Nuclear data sheets for  $A = 47$ , *Nucl. Data Sheets* **108**, 923 (2007).
- [20] L. G. Mann, D. C. Camp, J. A. Miskel, and R. J. Nagle, New measurements of  $\beta$ -circularly-polarized  $\gamma$  angular-correlation asymmetry parameters in allowed  $\beta$  decay, *Phys. Rev.* **139**, AB2 (1965).
- [21] J. Atkinson, L. Mann, K. Tirsell, and S. Bloom, Coulomb matrix elements from  $\beta$ - $\gamma$ (CP) correlation measurements in  $^{57}\text{Ni}$  and  $^{65}\text{Ni}$ , *Nucl. Phys. A* **114**, 143 (1968).
- [22] H. Behrens, Messung des asymmetrie-koeffizienten der  $\beta$ - $\gamma$ -zirkularpolarisationskorrelation an erlaubten  $\beta$ -übergängen, *Eur. Phys. J. A* **201**, 153 (1967).
- [23] J. Markey and F. Boehm, Fermi–Gamow–Teller interference in  $^{56}\text{Co}$  decay, *Phys. Rev. C* **26**, 287 (1982).
- [24] N. Severijns, D. Vénos, P. Schuurmans, T. Phalet, M. Honusek, D. Srnka, B. Vereecke, S. Versyck, D. Zákoucký, U. Köster, M. Beck, B. Delauré, V. Golovko, and I. Kraev, Isospin mixing in the  $T = 5/2$  ground state of  $^{71}\text{As}$ , *Phys. Rev. C* **71**, 064310 (2005).
- [25] P. Schuurmans, J. Camps, T. Phalet, N. Severijns, B. Vereecke, and S. Versyck, Isospin mixing in the ground state of  $^{52}\text{Mn}$ , *Nucl. Phys. A* **672**, 89 (2000).
- [26] J. J. Liu, X. X. Xu, L. J. Sun, C. X. Yuan, K. Kaneko, Y. Sun, P. F. Liang, H. Y. Wu, G. Z. Shi, C. J. Lin, J. Lee, S. M. Wang, C. Qi, J. G. Li, H. H. Li, L. Xayavong, Z. H. Li, P. J. Li, Y. Y. Yang, H. Jian *et al.* (RIBLL Collaboration), Observation of a strongly isospin-mixed doublet in  $^{26}\text{Si}$  via  $\beta$ -delayed two-proton decay of  $^{26}\text{P}$ , *Phys. Rev. Lett.* **129**, 242502 (2022).
- [27] F. P. Calaprice, S. J. Freedman, B. Osgood, and W. C. Thomlinson, Test of time-reversal invariance in the beta decay of  $^{56}\text{Co}$ , *Phys. Rev. C* **15**, 381 (1977).
- [28] P. Herczeg, The general form of the time-reversal non-invariant internucleon potential, *Nucl. Phys.* **75**, 655 (1966).